How to Cite:
AL-Adilee, K. J. K., & Hassan, H. M. (2022). Preparation, spectroscopic characterization and study of biological activity as anticancer of some compounds using a new azo-Schiff base ligand (N,N,O) derived from 2-amino-5-methyl thiazol. *International Journal of Health Sciences*, *6*(S4), 12002–12019. https://doi.org/10.53730/ijhs.v6nS4.11698

Preparation, spectroscopic characterization and study of biological activity as anticancer of some compounds using a new azo-Schiff base ligand (N,N,O) derived from 2-amino-5-methyl thiazol

Prof. Dr. Khalid Jawad Kadhim AL-Adilee
Department of chemistry, college of science AL-Qadisiyah University, Iraq
Corresponding author email: khalid.jawad@qu.edu.iq

Haider Mahdi Hassan
Department of chemistry, college of science AL-Qadisiyah University, Iraq
Email: zamilihaider6@gmail.com

***Abstract*---**The biological activity of the Co(III) complex of azo-Schiff bases derived from 2-amino-5-methylthiazole azo-Schiff bases was studied. Elementary examines, attractive instant volumes, spectroscopy (IR, electronic, 1 H NMR, and XRD), then thermogravimetric investigations described the azo-Schiff bases and their mineral complexes. For the cobalt complex, an octahedral geometry has been proposed. Thermal and infrared data of the mineral complexes confirmed the presence of the collected water. Schiff bases and mineral complexes have been tested for their anti-cancer properties

***Keywords*---**Thiazol, azo-Schiff, anti cancer, hydroxe benzyldehyd, amino phenol.

Introduction

Thiazoles and thiazole derivatives were developed via different heterocyclic chemistry routes[1]. The synthesis of thiazoles was started by Hofmann and Hantzsch & Coworkers[2]. There are two core ways for synthesizing thiazole: addition reaction and cyclization reaction[3]. Chemically, thiazoles (1,3 thiazole) occupy an important position due to their unique 5-membered heterocyclic ring structure[4]. Many heterocyclic products contain thiazoles and thiazole derivatives,

such as antibiotics, antimicrobials, anticancer medications, anti-inflammatory drugs, and anticonvulsants[6].

Thiazole is a strong pale-yellow liquid by a boiling point of 116 -118 ºC, solvable in ehtanol and ether but abstemiously solvable in water[7]. The heterocyclic ring of thiazole contains a delocalisation of 6 π electrons consistent to Huckel's rule from the lone pair electrons, which is the sulphur atom[8]. A thiazole is a 3-dimensional compound that has been synthesized from synthetic, natural plants, marine organisms, as well as by using green chemistry methods (which includes the use of green solvents, catalysts, solid-phase preparation, microwave irradiation, and ultrasonication)[9].

Materials and Methods

Chemicals and solvents

Alchemical used in this study are of pure grade (BDH\Adrich), including 2-Amino-5-methyl thiazol Sodium nitrite ($NaNO_2$), HCl, 3-Amino phenol2-hydroxybenzyldehyde, sodium hydroxide, ethyl alchol , Glacial Acetic acid, Ammonia concentrated, dimethylsulphoxide (DMSO), $NiCl_2.6H_2O$, $CuCl_2$. 6H2O.$ZnCl_2$ and distilled water.

Physical measurements

The EA 300 (CHNS) Component analyzer is used to control ligand (HLH) rudimentary microanalyses. The 1 H and 13C NMR ranges are got using a Broker 400 MHZ spectrometer with DMSO-d6 as the solvent and TMS as the interior orientation. The electric ranges remained got in complete ethyl alcohol is by a quartz cuvette with a 1 cm trail distance of 200–1100 nm on a T80-PG two beam (UV-Vis) spectrophotometer. A Shimadzu Agilent Technologies 5973C mass spectrometer was used to record ligand (BIAB) mass spectra (70 eV). A Bestec Aluminium anode-Germany was used to perform X-ray diffraction (XRD) observations. X-ray diffractometer in the range of (20–80) with (Cu K) radiation (14 1.5418 A). A Shimadzu 8400 S recorded FT-IR spectra (KBr disks, 4000–400 cm1). the field Images was taken using a scanning electron microscope (FE-SEM). TESCAN MIRA3 The Stuart instrument, developed by SMP, was used for the analysis. The melting point or decay temperature of the substance is recorded. Capillary tube, ligand A pH meter is used to take the readings PW 9421 by Philips. PerkinElmer Chem Bio Draw software is used to develop the chemical, which was subsequently optimiz using PerkinElmer ChemBio3D software.

Synthesis of novel azo-Schiff base ligand (HLH)

Thiazole azo ligand preparation

First step: 1.7 g (0.01) mol of 2-amino-5-like thiazole is dissolved in the mixture consisting of (35 ml purified water with 5 ml of focused hydrochloric acid) and completely dissolve, then the prepared mixture is cooled to a degree (3-0) m and add to the mixture (0.75) g (0.01 mol) of sodium nitrite solution (NaNO2) dissolve in 35 ml of distilled water, droplet thru droplet with incessant stirring and noting

that the temperature did not increase above 4 o C, where the discoloration of the solution was observed. The resulting yellow and bubbles continuously exit from the solution. After that, the prepared solution was left to settle for 15 minutes in order to complete the nitrification process.

The second step: a weight of 1.2 g (0.01) mol of 3-aminophenol was taken and dissolve in 30 ml of pure ethanol, then 15 ml of NaOH 10% sodium hydroxide is added to it, then the mixture is cooled. After that, the mixture prepared in the first step is added to the mixture prepared in the second step, drop by drop. The color of the solution is observed in a dark red color. The mixture was stirred for one 40 minutes at a temperature of (0-0) C, then 100 ml of distilled water was added to it, then the solution was filtered and the precipitate is washed in distilled water several times and then recrystallized using absolute ethyl alchol, then the precipitate is dried and kept in an opaque bottle, for a few hours. In this method, the compound 2-[2--(5-methyl) azo]-5-aminophenol is prepared.

Preparation of azo ligand - Schiff base

The azo ligand- Schiff base (HLH) remained ready through the concentration reaction of 2-hydroxybenzaldehyde and the azo compound prepared in paragraph 2.-3-1-a) dissolve 1.2 g (0.01) mol of 2-hydroxybenzaldehyde in 40 ml ethanol Complete is varied by a solution of 3 g (0.01) of azo compound dissolved in 50 ml of absolute ethanol also with the addition of four droplets of glacial acetic acid, as a catalyst, followed by escalation of the mix by heat for (4-6) hours after which the reaction mixture was left to cool Then it was decanted ended ice smithereens of distilled water, where reddish-purple crystals seemed. These crystals are filtered, dried, and recrystallized in hot ethyl alchol for a few hours. The proportion of the prepared product is calculated and its melting point was measured to obtain an azo ligand - Schiff base (HLH), and the diagram (1-) 2) Below are the processes of denitrification and coupling.

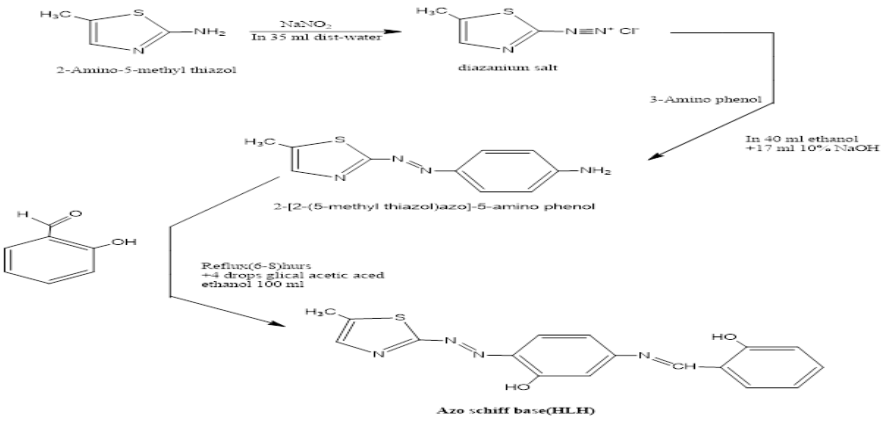

Synthesis of complexe

Cobalt(II) metal salt ion complexes were prepared by a molar ratio of [1:2] [M:L] by add the desired mass of all ligand (0.001) mol of the Synthesis ligand and dissolve in 25 ml of pure and absolute ethyl alcohol flush slowly with rousing. Continuous

to the mineral solution (0.0005) mol of metallic chlorides melted in 25 ml of bumper solution with continuous stirring for 30 minutes at a temperature of 60 ° C, in dark colors, and the solutions are left for 24 hours to complete obtaining the sediment, then the sediment is filtering and washing numerous eras With non-ionic water and formerly by a minor quantity of ethyl alcohol solvent to remove the unreacted organic matter and then recrystallize by complete ehyl alcohol.s

Table (1): - physical properties and component examination for original azo-Schiff base ligand (HLH), their metallic complexe, and the molar ratios additional from the ligand and meta

Compound	Colour	m.p °C	Yield (%)	M.et (M.wt)	Elemental analysis (%):calcd. (Found)				
					C%	H%	N%	S%	M%
Ligand= HLH	Dark purplish	143	82	$C17H14N4O_2$ S (338.39)	60.340 (61.79)	4.170 (5.33)	16.557 (17.64)	9.474 (9.95)	-
$[Co(HLHL)_2]$ Cl $.H_2O$	Brown yellowish	261	67	$C_{34}H_{28}N_8O_5S_2CoCl$ (787.152)	51.879 (52.56)	3.585 (3.77)	14.235 (15.85)	8.145 (9.26)	7.476 (8.23)

Result and Discussion

Characterization of azo dye ligand (LH) and its metal Complexe

At room temperature, the produced compounds are unchanging in air and dampness. They are not soluble in water. Solvable in Dimethyl sulfoxide is methanol and ethanol, and dimethylformamide (DMF). The complexes' logical outcomes agreed with the stoichiometry predicted[10].

Mole ratio method

The metal:ligand ratio [M:L] is calculated using the molar ratio way in absolute ethyl alcohol as a solvent with unlike maximum values for the complex[11]. The assay of the metal complex composition was completed using UV-visible spectrophotometry at continuous attentions and wavelengths of the metal ion (maximum) and increase the volume of the ligand solution (0.25 ml each, adding up to 3.5 ml). The increase color intensity of the complex mineral solution and prolonged color stability at the point of intersection are strong indicators of the formation of multifaceted minerals at the typical ratio. The results indicated that the ligand interacted with metallic ions in a mole ratio of [2:1] metal to ligand [M:L], which is consistent with our previous findings[12].

Molar conductivity

In DMF and EtOH solutions, the cobalt (Co)(III) complex had a molar conductivity value of 37.82 (s. cm2 mol-1). The chloride ion was determined using the Mohr method[13]. that are in the range of nonelectrolytes (18). No ions were found outside the coordination domain, which means that chloride ions may or may not be present inside. Chemical examination showed that addition of AgNO3 solution

does not precipitate Cl ions. The electrolyte properties were not observed in any of the complexes.

^{1}H NMR studies

^{1}H- NMR spectroscopy of the ligand azo-Schiff base (HLH)

The ligand (HLH) is diagnosing using 1 H-NMR proton nuclear magnetic resonance spectroscopy using DMSO-d-6 dimethyl sulfoxide as a solvent[14,13], as TMS used as a standard reference [15]. The H1-NMR proton spectrum of the ligand showed a single signal at chemical displacement δ = (11.11,9.86) ppm, which belongs to the hydroxyl group at position 15 and 24, respectively. And it showed multiple, double and double signals at the chemical shift ppm 7.65-6.52 δ= belonging to the aromatic ring proteins (thiazole and the benzene ring) at positions 22,21,20,19,14,13,11,2 respectively as it showed a sign at the ppm chemical shift 8.94 δ = back to the azomethine group (N = CH) back to position 17 and finally a signal looked at the chemical displacement δ = 2.30 ppm back to the like group (-CH3) at position 6

The figure below shows the spectrum of HLH. Protein

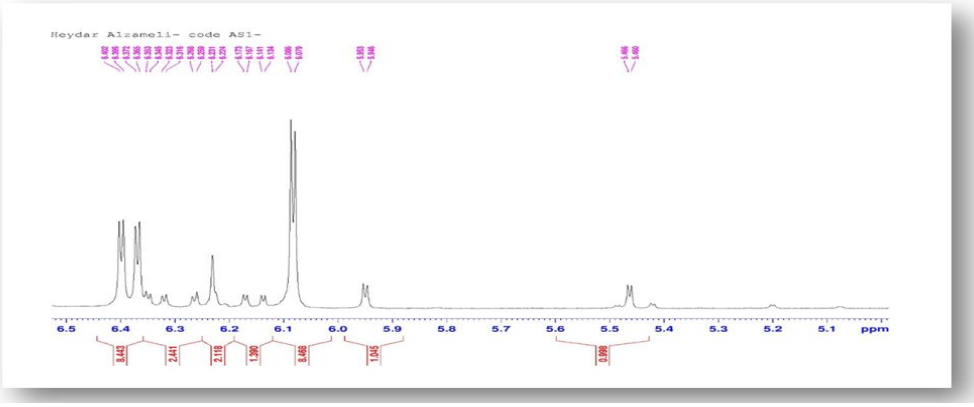

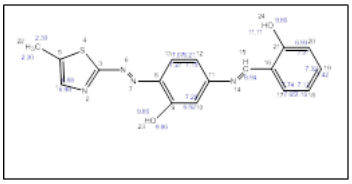

The NMR proton spectrum of the coplat (III) complex:- $[Co(HLH)_2]Cl.H_2O$

The H1-NMR spectrum of the cobalt complex show a one beam at chemical dislocation δ=2.08 ppm, which is owing to the attendance of the methyl group at positions 6 and 31 of the thiazole ring, and presented a solitary ray at chemical dislocation δ=3.72 ppm, which is due to the presence of the two methyl groups at positions 24 , 25 , 49 and 50 in the aromatic circle, though the multiple groups at the chemical dislocation δ = 6.79 ppm refer to the two aromatic ring protons at

positions 11 , 36, and also multiple bands looked from the chemical distraction δ = 7.10 ppm that belong to the two aromatic ring protons at positions 13 and 38, Also, a single beam seemed at the chemical dislocation δ=7.20-7.22 ppm and it belongs to the aromatic ring protons at positions 19, 21, 44 and 46, while the two single beams at the chemical dislocation= 7.62 ppm δ that energies spinal to the two aromatic circle protons at positions 4 and 29, respectively, and the range showed a single band at the chemical displacement δ = 7.68 ppm that goes back to the two aromatic ring protons at positions 10 and 35, and the spectrum showed bands equal to δ= 7.90-7.92 The ring protons for positions 18, 22, 43 and 47, though the single beam at chemical dislocation δ = 8.00 ppm belongs to the proton of the N = CH group at positions 41 and 16, though the spectrum showed beams at chemical dislocation δ = 3.76 ppm fitting to the protons of the solvent DMSO-d6. (16-3) NMR proton spectrum of the cobalt(III) complex.

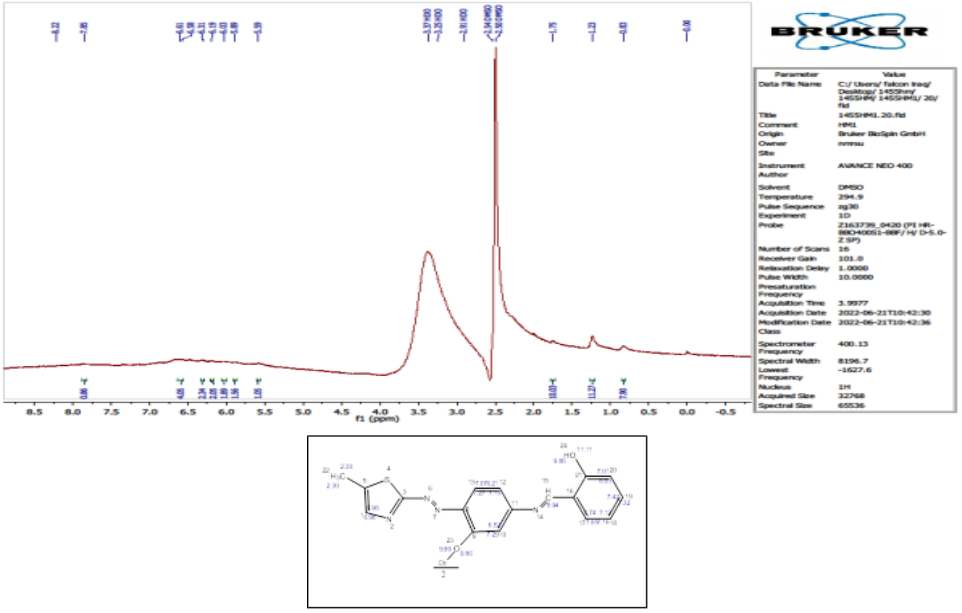

Infrared spectra studies

This region is characterized by the fact that it contains several or greatest of the preoccupation groups that fit to the lively collections in the ranges of licandene and their metal complexes, counting collections and (C = N), (N = N), (C = C) and additional real groups, in addition to the vibrations that return For the (M-N) bond (metal-nitrogen) and the M-O bond (metal-oxygen), through likening the ranges of the metallic complexes below education in this district of the spectrum with the spectra that belong to the free ligand, it is noticed that the bands shifted, either towards lower frequencies or higher incidences[16,17]. To the appearance of novel groups that are not current in the ranges of Likando, which indicates the occurrence of synergy We shall discuss in part the ligand beams that are affected by coordination with the metal ion, as it gave the infrared spectrum of the ligand with the cobalt complex according to the table below[18].

Fig.(2). FT-IR spectrum of the ligand (LH) and its metal complexes

Group	Ligand (LH)	Co(II) Complex
υ- OH	3300m.br	3311m.br*
υ- (CH)aliph	2966_s	2983_s
υ- (CH)arom	3093 s	3153_S
υ- (C=N)	1599m	1597_m
υ- (N=N)	1537s	1489s
υ- (C=C)	1402_m	1402_m
υ- (C-S)	1384s	1300m
υ-(C-N)	1247s	1139s
υ-(C-O)	……	1220_S
υ-(M-O)	……	470w
υ-(M-N)	…….	520w

S=strong, m=medium, w=weak, br=broad ,*=(H_2O) outside of sphere coordination

The figure below shows the infrared spectrum of the HLH ligand.

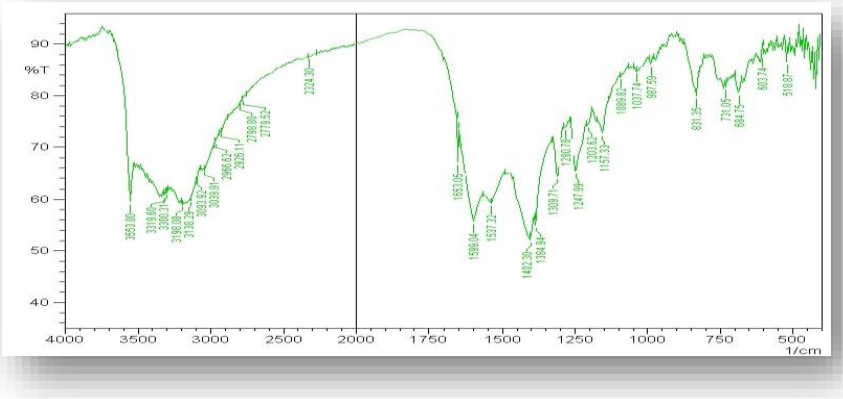

The figure below shows the infrared spectrum of the Co(III) cobalt complex.

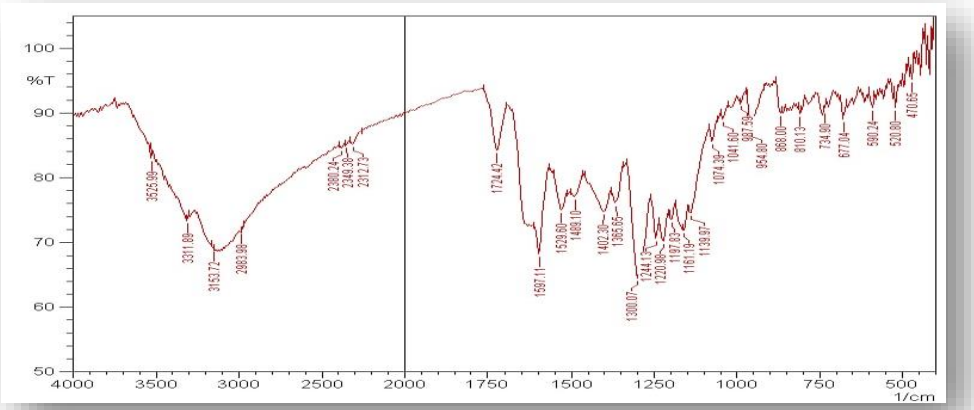

Electronic spectra studies

Electronic spectra of free ligand (HLH)

The spectrum of the ligand gave five peaks, the first at frequency 476 nm (49,019) (cm-1) is related to the electronic transition (n →π*), the second peak at the frequency 271 nm 36900 (cm-1) belongs to the electronic transition (n — π*) and the third peak At the frequency (260) nm (38465 cm-1) belonging to the electronic transmission (π — π*) of the azo group (N = N) and group (C = N), the fourth and fifth peaks, respectively, appeared at the frequency (206,204) nm (48543, 49019 cm-1) belonging to the (π→π*) electron transfer of the (C=C) bond in the thiazole ring and the aromatic ring[19,20]

Electronic spectra of Co (II)- complex

complex, the UV-visible spectrum of the cobalt(II) complex showed four absorption peaks, the first peak at frequency 524 nm 19083.97 (cm-1) due to the electron transition (A1g →1T2g (F) (υ11) and the second peak at frequency 241 nm 41493.78) cm -1) It goes back to the electronic transition (A1g →1T1g (F) (υ11), what are the third and fourth peaks, respectively at frequency (217, 202 (46082.95 nm), 49504.95 cm-1) due to the transition inside the ligand and its proposed geometry is octahedral Regular and its hybridization is d2sp3.

Table (3): Electron transfer spectra of the azo ligand - Schiff (HLH) and cobalt complex

Compounds	λ_{max} (nm)	Absorption Bands(cm^{-1})	Transitions	μ_{eff} (B.M)	Geometry	Hybridization
Ligand=HLH	476	21008.41	n—π*	-	-	-
	271	36900.37	π —π*			
	260	38463.54	π —π*			
	206	48543.96	π —π*			
	204	49019.61	π —π*			
$[Co(HLH)_2]Cl.H_2O$	524	19083.97	$^1A_1g \rightarrow {}^1T_2g$	Dia	Octahedral (Regular)	$d^2 sp^3$ (Low spin)
	241	41493.78	$^1A_1g \rightarrow {}^1T_2g$			
	217	46082.95	Inter ligand			
	202	49504.95	Inter ligand			

Figure No. (4). Electronic spectra of the ligand and the cobalt complex.

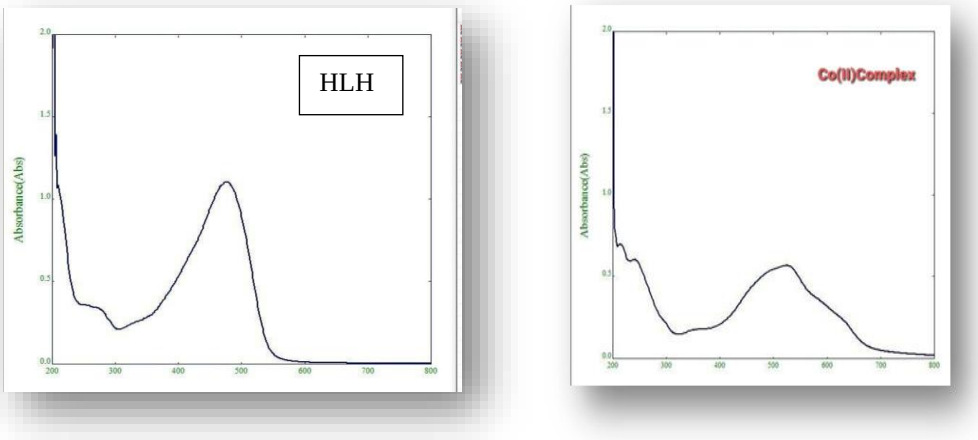

Field-emission Scanning Electron Microscop

Emission-field skimming electron microscopy (FE-SEM) is using to education the mineral construction, surface structure, shape and size of the particles, and crystal distribution. The scan electron microscope technique is adopting in the emitted field at a cross-sectional coldness of 200 nm and exaggeration strength KX Mag = 20.00, and Image J program is using to calculate particle sizes and some properties[21].

The surface properties of the azo-base-Schf ligand (HLH) units and its metal complexes with metal ions are studying From the crystalline form of the atoms and assemblies by scan electron microscope technology and finished the FESEM analysis copy of the Ligand (HLH), where it becames pure to us that its form is varied crystals and the regular size is 57.42 nm. As for the analysis image . Whereas, the cobalt (III) complex shape showed by FESEM analysis of small crystals with a heterogeneous surface size and a particle size of 87.15 nm.

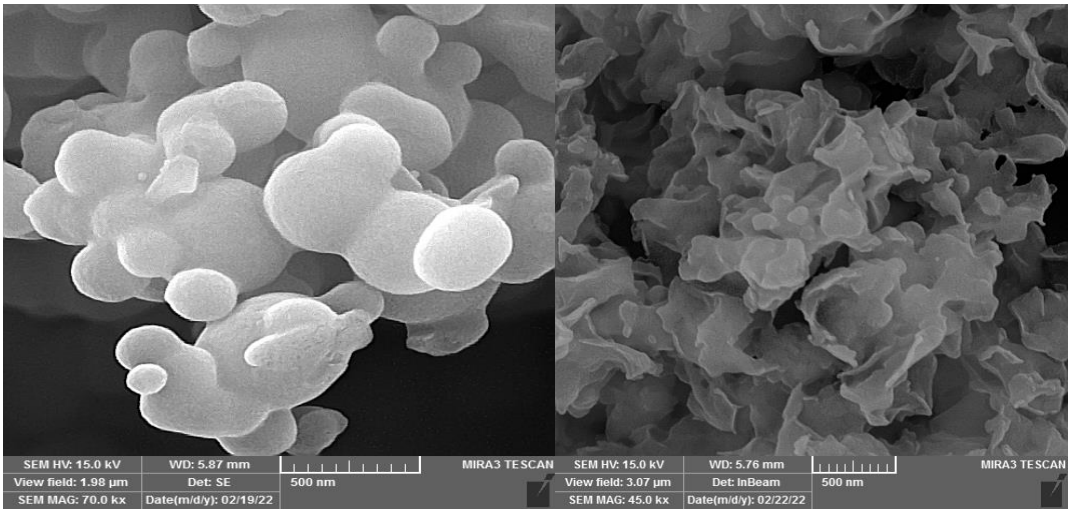

HLH Co(III)Complex

X-ray diffraction study (XRD)

The ligand, H L H, and its metallic complex in its hard national were examined using X-ray deflection within (angular range) 5°-80°))θ2 in order to distinguish certain physical possessions, mineral constructions and mineral sizes. Micro strains and Displacement thickness were too intended.) to discovery out the degree of its cleanliness. and the flaws in the mineral construction when changing the ligand into its metal complex There are certain deflection mountains for which a appraisal happens for the next reasons: Micro strain, such as the absence of mineral frame distortion, and mineral criticizing happens As a consequence of the misrepresentations that happen in the mineral and the mineral scope area ((Domain size of the Crystal and Distribution of domain))[22,23]. The Debye-Scherr reckoning was also used Debye-Scherer to compute the mineral size of Leyland (HL H) and its metallic complex as follows[24].

$$D = \frac{k\lambda}{\beta \cos\theta}$$

where D = average crystal size. k = shape factor, whose value is usually about 0.9, λ represents the wavelength of the X-rays and its value is CuKα = 1.54056 A°, β = the total width of the FWHM, θ is the deflection angle. The next calculation was too used to compute the micro-compliance[25].

$\delta = 1/D^2$
Where δ represents the atomization density and D = the average crystal size

It remained exposed through X-ray spectra (XRD) the clear change in the before stated statistics of mineral size, micro-compliance, thickness of closures, and space amid mineral heights of ligand and its ready metal complex. It remained originate that the advanced the mineral size, the inferior the micro plasticity and the lower the atomization density, therefore plummeting the flaws of the mineral In adding, it remained experiential that the ligand and its metallic complex must a ounce size of less than 100 nm, which is within the nanoscale.

compound	Pos. [2Th]	Height [cts]	FWHM [2Th]	d-spacing [A]	Rel. Int [%]	Tip Width [2Th]	Crystal lit Size D (nm)	Dislocation Density σ*10-3 (nm)2	Microstr Ain ε * 10-3
HLH	20.1467	387.23	0.3149	4.40765	41.19	0.3779	26.34907401	1.44035414	416.6431046
	21.4379	152.31	0.1771	4.14500	16.20	0.2125	46.85123804	0.45557287	416.7054047
	24.5684	570.72	0.3346	3.62349	60.71	0.4015	24.79772144	1.62620932	416.685717
	25.8986	940.11	0.2558	3.44032	100.00	0.3070	32.43682075	0.95043727	416.6113811

	27.9283	280.79	0.2165	3.19474	29.87	0.2598	38.32492933	0.68082779	416.6659528
	30.0400	106.35	0.3149	2.97480	11.31	0.3779	26.34907401	1.44035414	416.6431046
	33.1001	94.64	0.1673	2.70644	10.07	0.2007	49.59567124	0.40654856	416.7908045
	36.1882	47.70	0.4723	2.48226	5.07	0.5668	17.56778959	3.24015485	416.6338641
	37.4040	43.07	0.6298	2.40433	4.58	0.7557	13.17432216	5.76160447	416.6937077
	39.3348	23.02	0.4723	2.29064	2.45	0.5668	17.56778959	3.24015485	416.6338641
Co(II)-complex	20.7131	235.79	0.1870	4.28840	68.25	0.2244	44.3708696	0.50793029	416.6661341
	31.2447	185.02	0.1968	2.86279	53.56	0.2362	42.16133586	0.56256314	416.595515
	32.9750	345.45	0.1968	2.71642	100.00	0.2362	42.16133586	0.56256314	416.595515
	35.8692	73.67	0.9446	2.50360	21.33	1.1336	8.783572442	12.96157046	416.6236707
	37.7484	259.23	0.2165	2.38318	75.04	0.2598	38.32492933	0.68082779	416.6659528
	39.2399	141.99	0.2263	2.29596	41.10	0.2716	36.66524622	0.74385928	416.6045218
	42.1838	205.17	0.1968	2.14229	59.39	0.2362	42.16133586	0.56256314	416.595515
	43.4741	229.63	0.2263	2.08166	66.47	0.2716	36.66524622	0.74385928	416.6045218
	54.6028	81.59	0.2558	1.68081	23.62	0.3070	32.43682075	0.95043727	416.6113811
	57.8988	138.83	0.3000	1.59140	40.19	0.3600	27.65775859	1.30727223	416.6652959

Figure (5):- X-ray diffraction spectrum of the azo base-Schiff ligand (HLH) and its metallic complex

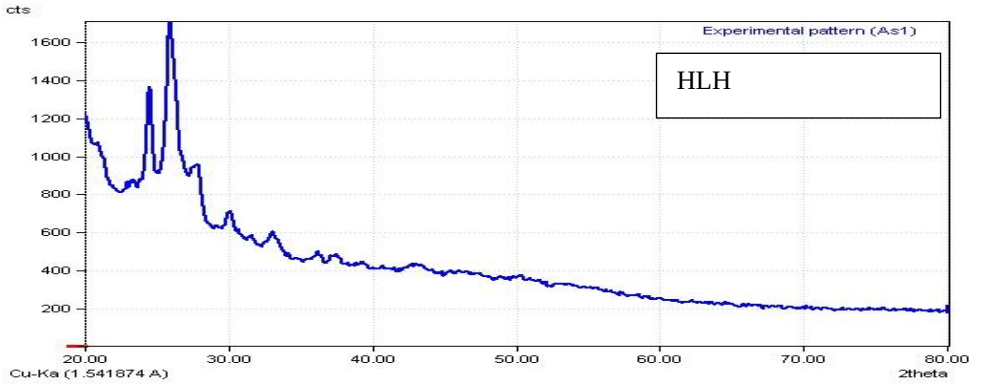

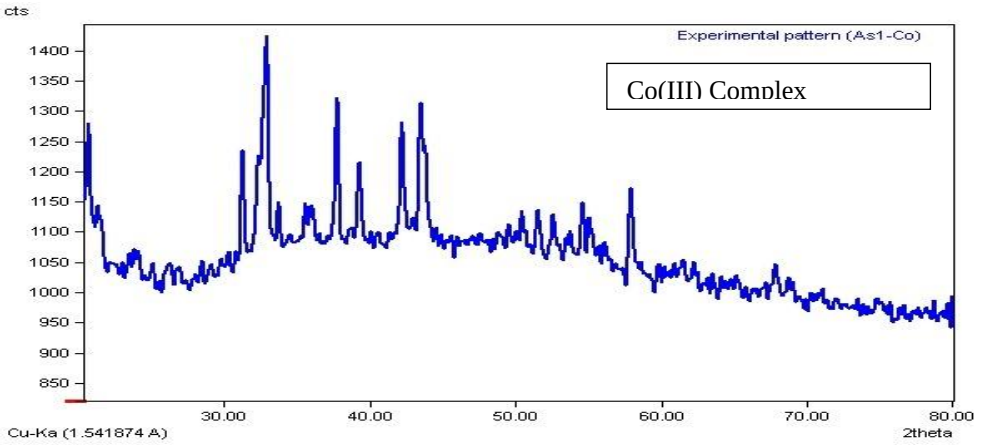

Anti-cancer effect
Cytotoxicity by use Assays (MTT)

In this study, two cell lines, colon cancer cancer cell line (Caco-2) and normal neonatal hemolysis cell line (HdFn) were used for comparison and for the purpose of demonstrating their effectiveness on human body cells and the extent to which they can be used as cancer drugs. Cancer cells and healthy cells of each type, as the test (MTT) was used for the biological examinations of all cells.

The results showed the appearance of toxic effects on the growth of cancer cell lines, and less effect on healthy cells of ligand concentrations (HLH) and its metal complex, and the possibility of using them as potential drugs for various cancers. or their growth has stopped [26,27]. The toxicity of cancer cells varied from one cell line to another, and this is due to the different cells of the cell lines Cancer and normal in their receptors, as the thiazole molecule has the inhibitory ability against cancerous and normal cells by affecting certain receptors on the surfaces of these cells and through those receptors the cells are responsive to programmed cell death apoptosis[28].

The results also showed that the type and concentration of the compound used are important factors in determining the percentage of cytostatics. It was found that increasing the concentration of the prepared compounds under study increases the rate of inhibition of cell growth in cancerous and normal lines and this phenomenon is called dose dependent, and this is consistent with what many scientists have reached [29] where the rate of effectiveness increases with increasing concentration and as Shown in the figures below We also note that the higher the concentration, the higher the number of killed cells and the lower the number of living cells, knowing that the process of interaction of different concentrations of the prepared compounds is repeated three times (called three replicates).

Colon cancer cell line (Caco-2)

Effect of ligandthiazole (HLH) on the growth of colon cancer cell lines (Caco-2) as well as healthy cells (HdFn)

The results in Table (6) showed the effect of the thiazole ligand (HLH) on the growth of colon cancer cell lines (Caco-2) as well as healthy cells (HdFn). The lowest percentage of cell growth was found at 25 µg/ml and the highest at 200 µg. \ml for colon cancer cell lines (Caco-2) as well as normal cells (HdFn). For information, normal cells were used To compare with colon cancer cells and to show the extent to which it can be used as a drug. It was noted that the levels of inhibition of the ligand (HLH) differ according to the type of cell line, as the number of live cells remaining after interaction with the thiazole ligand ranges between (94.41%-49%) for cells of the colon cancer cell line (Caco-2), and between (94.95% - 80.05%) for normal cell line (HdFn) cells. The highest inhibition of lycand was also observed (HLH) of the colon cancer cell line (Caco-2) at a concentration of 200 µg/ml, as the percentage of inhibition after interaction with the ligand ranged 51.15%, while it was noted that the highest inhibition of the ligand (H2L) of the normal cell line (HdFn) at the same concentration in The percentage of inhibition after the reaction with the ligand ranged from 16.74%.

Table (5) shows the effect of the thiazole ligand (HLH) on the growth of colon cancer cell lines (Caco-2) and comparing it with the normal cell line (HdFn) for the same concentration using MTT test for a period of 24 hours

Concentration (µg/mL)	H2L					
	Cancer line cells			Normal line cells		
	Caco-2			HdFn		
	Cell Viability		% Cell Inhibition	Cell Viability		% Cell Inhibition
	Mean	SD		Mean	SD	
0	100.0000821	1.916969709		100.0049425	1.606326455	
25	94.41	3.06	5.59	94.83	2.10	5.17
50	75.31	4.75	24.69	94.95	1.86	5.05
100	65.70	0.35	34.30	92.82	1.01	7.18
200	48.85	4.68	51.15	83.26	1.12	16.74
400	49	3.54	51	80.05	0.97	19.95
IC_{50}	65.4			151.1		

The effect of the cobalt complex Cl.H2O[Co(HLH)2] on the growth of colon cancer cell lines (Caco-2) as well as healthy cells (HdFn)

The results in Table (6) showed the effect of Cl.H2O[2(H2L)Cu] complex on the growth of colon cancer cell lines (Caco-2) as well as healthy cells (HdFn), where the lowest percentage of cell growth inhibition was found at a concentration of 25 µg/ml. The highest inhibition rate at a concentration of 200 µg/ml was for colon cancer cell lines (Caco-2) as well as normal cells (HdFn). For information, normal cells were used to compare with colon cancer cells and to indicate the possibility of using it as a drug. It was noted that the inhibition rates of the copper complex vary according to the type of cell line, as the number of remaining living cells

varies After the reaction with the thiazole ligand, it ranged between (93.99%-48.70%) for the cells of the lung cancer cell line (Caco-2), and between (95.06%-73.03%) for the cells of the normal cell line (HdFn). The highest inhibition of the copper complex was observed for the colon cancer cell line (Caco-2) at a concentration of 400 µg/ml, as the percentage of inhibition ranged after interaction with the ligand 51.30%, while it was noted that the highest inhibition of the ligand (HLH) was for the normal cell line (HdFn).) with the same concentration in the above, as the percentage of inhibition ranged after the reaction with the ligand is 26.97%.

Table (6) shows the effect of cobalt complex on the growth of colon cancer cell lines (Caco-2) and comparing it with normal cell line (HdFn) for the same concentration using MTT test for a period of 24 hours

Concentration (µg/mL)	$Cl.H_2O\ ]Co(HLH)_2[$					
	Cancer line cells			Normal line cells		
	Caco-2			HdFn		
	Cell Viability		% Cell Inhibition	Cell Viability		% Cell Inhibition
	Mean	SD		Mean	SD	
0	100.0000821	1.916969709		100.0049425	1.606326455	
25	93.02	1.87	6.98	95.06	1.24	4.94
50	85.19	0.83	14.81	95.45	0.24	4.55
100	76.47	2.57	23.53	94.52	0.71	5.48
200	61.08	4.64	38.92	84.49	3	15.51
400	48.70	71ر8	51.30	73.03	1.16	26.97
IC_{50}	178.8			206		

Inhibition Concentration Fifty (IC50)

One of the important matters that must be mentioned and was reached by the tests conducted on the thiazole compound (HLH) and its metal complexes and between the cells of the lung cancer cancer lines (Caco-2) and the human normal cell line (HdFn) is the so-called half inhibitory concentration. Concentration Fifty) [31,32], which symbolizes (IC50), as this concentration kills nearly half of the cells. We note that in the case of interaction of the thiazole ligand (HLH) with the colon cancer cell line (Caco-2), the half inhibitory concentration is 65.4 µg/ml, where we note that the half inhibitory concentration (IC50) is within the range of concentrations taken and compared to cells of the normal line (We note that the half inhibitory concentration in the case of the interaction of the ligand (HLH) with the normal cell line (HdFn) is 151.1 µg/ml, and this is a good result, meaning that the ligand kills cancer cells and has a slight effect on normal cells because they need a high concentration until Half of them are killed, and this result is important in this field of our research, as shown in the figure below(6).

We also note in the case of the interaction of the cobalt complex Cl.H2O[Co(HLH)2] with the colon cancer cell line (Caco-2), the half-inhibitory concentration equals 178.8 µg/ml, where we note that the half-inhibitory concentration (IC50) is within the range of the taken concentrations. In comparison with the cells of the normal line (HdFn), we note that the half

inhibitory concentration in the case of interaction of the cobalt complex with the normal cell line (HdFn) is equal to 206 µg/ml, and this is a good result, meaning that the cobalt kills cancer cells and has little effect on the normal cells because they need to a high concentration until it kills half of it, as shown in the figure(7).

Figure (6):- represents the relationship between the half-inhibitory concentration (IC50) of the HLH ligand) with the tumor cell lines (Caco-2) and the normal cell line (HdFn)

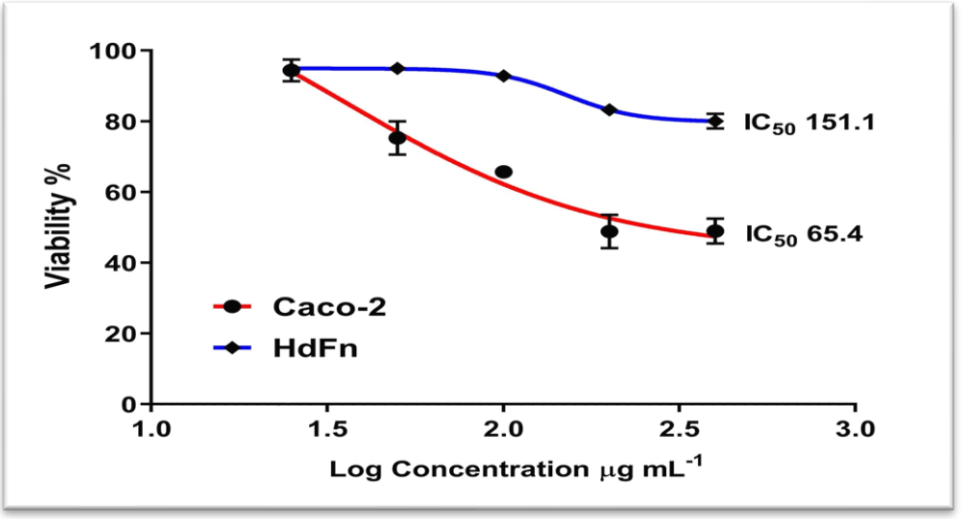

Figure (7):- represents the relationship between the half inhibitory concentration (IC50) of the cobalt complex (Co(III) with the cancer cell lines (Caco-2) and the normal cell line (HdFn)

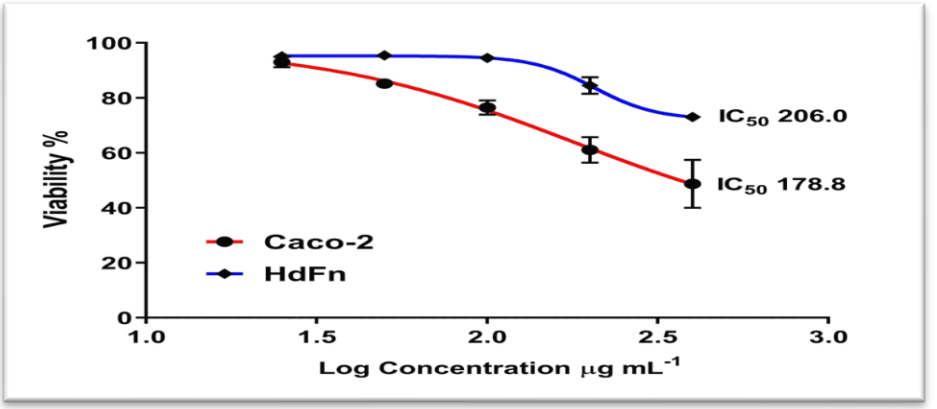

Conclusions

A thiazole-derived ligand has remained ready, and the complexes of this attachment are azure divalent mixes. They were resolute by execution numerous examines, such as UV- and IR spectroscopy, mass spectrometry, attractive compassion, XRD techniques, FE-SEM, and molar conductivity. It is showed that complexes have dissimilar constructions and forms**.** The ligand is synchronized to

the metal by three binding sites: the nitrogen of the azo collection, the nitrogen of the thiazole ring, and the oxygen of the hydroxyl group after losing its proton. The molar conductivity consequences exposed a chloride ion outdoor the organization province. FE-SEM images of the as-prepared metallic complexes presented that attachment and its complexes are nanoparticles that can be used as a cancer therapy. The biological activity and toxicity of ligand and its compounds were performed on infected cells using colon cancer cell lines and compared with normal human umbilical vein endothelial cell lines. (Caco-2). It can be concluded that The azo-Schiff ligand and the cobalt compound have cytotoxic properties against lung cancer.

References

1. Alkhafaji, Mohammed Nawfal Abdul Maged, & Nagham Mahmood Aljamali. "Preparation of Benzothiazole-Formazane Reagents and Studying of (Spectral, Thermal, Scanning Microscopy, Biological Evaluation)." *International Journal of Pharmaceutical Research* 13.1 (2021).
2. Anjana, A., & Chacko, A. T. (2014). Prevalence and correlates of functional limitation among elderly in Kerala. *International Research Journal of Management, IT and Social Sciences*, *1*(1), 22-29. Retrieved from https://sloap.org/journals/index.php/irjmis/article/view/249
3. Bait, S., Shinde, S., Adivarekar, R., & Sekar, N. "ESIPT Core Containing Benzothiazole and Benzimidazole Based Fluorescent Acid Azo Dyes for Protein Fiber: Synthesis, Spectral
4. Cavalluzzi, Maria Maddalena, "Lubeluzole: from anti-ischemic drug to preclinical antidiarrheal studies." *Pharmacological Reports* 73.1 (2021): 172-184.
5. Characteristics, and Fastness Evaluation." *Polycyclic Aromatic Compounds* (2022): 1-22.
6. Chuan Lim, Eldin Wee, & Ruili Feng. "Agglomeration of magnetic nanoparticles." *The Journal of chemical physics* 136.12 (2012): 124109.
7. Dakheel, Haitham Kadhim, Wafaa Fadhil Abbas, & J. Khalid. "Al-Adilee." Synthesis, Anticancer, and Antioxidant Activities of New Azomethine Dye and Its Co (Iii) Complex."." *International Journal of Applied and Natural Sciences (IJANS 9.5* (2020): 53-62.
8. Gu, P. Y., Xu, Q. F., Ge, J. F., Liang, Z., Lu, J. M., & Wang, L. H. "ATRP of MMA initiated by 2-bromoisobutyric acid 4-(2-benzothiazole-2-yl-vinyl)-phenyl ester (BPBVE) and its fluorescent property in the presence of metal ions." *e-Polymers* 10.1 (2010).
9. Javed, Irfan, Seung Wook Baek, & Khalid Waheed. "Effects of dense concentrations of aluminum nanoparticles on the evaporation behavior of kerosene droplet at elevated temperatures: The phenomenon of microexplosion." *Experimental thermal and fluid science* 56 (2014): 33-44.
10. Karalı, N., Güzel, Ö., Özsoy, N., Özbey, S., & Salman, A. "Synthesis of new spiroindolinones incorporating a benzothiazole moiety as antioxidant agents." *European journal of medicinal chemistry* 45.3 (2010): 1068-1077.
11. Korkmaz, Adem, & Ercan Bursal. "Benzothiazole sulfonate derivatives bearing azomethine: Synthesis, characterization, enzyme inhibition, and molecular docking study." *Journal of Molecular Structure* 1257 (2022): 132641.

12. Lemos, Valfredo A., Miguel de la Guardia, & Sérgio LC Ferreira. "An on-line system for preconcentration and determination of lead in wine samples by FAAS." *Talanta* 58.3 (2002): 475-480.
13. Leoni, M., Di Maggio, R., Polizzi, S., & Scardi, P. "X-ray Diffraction Methodology for the Microstructural Analysis of Nanocrystalline Powders: Application to Cerium Oxide." *Journal of the American Ceramic Society* 87.6 (2004): 1133-1140.
14. Li, Qianqian, "Luminescent copper (I) complexes bearing benzothiazole-imidazolylidene ligand with various substituents: Synthesis, photophysical properties and computational studies." *Polyhedron* (2022): 115785.
15. Lv, W., Fu, B., Li, M., Kang, Y., Bai, S., & Lu, C. "Determination of IC50 value of anticancer drugs on cell by D2O-single cell Raman spectroscopy." *Chemical Communications* 14 (2022).
16. Ma, Tao, "Design, synthesis and properties of hydrogen peroxide fluorescent probe based on benzothiazole." *Bioorganic Chemistry* (2022): 105798.
17. Mohamed, T. Y. "Synthesis and Spectral Studies of Co (II), Cu (II) and Fe (III) Ions with 2 (2-Hydroxynaphthyl azo-) Benzothiazole." *Egyptian Journal of Chemistry* 57.1 (2014): 1-10.
18. Mohammed, Zahraa Kadhim, Hassan H. AL-Saeed, & Anees K. Nile. "Synthesis, reactivity and applications of aryl azothiazoles derivative." *International Journal of Advanced Research* 5.7 (2017): 2426-2496.
19. NA, Naser, & Kahdim KH. "Synthesis and characterization of an organic reagent 4-(6-bromo-2-benzothiazolylazo) pyrogallol and its analytical application." *Journal of Oleo Science* 61.7 (2012): 387-392.
20. Nagaraju, B., Kovvuri, J., Kumar, C. G., Routhu, S. R., Shareef, M. A., Kadagathur, M., & Kamal, A. "Synthesis and biological evaluation of pyrazole linked benzothiazole-β-naphthol derivatives as topoisomerase I inhibitors with DNA binding ability." *Bioorganic & medicinal chemistry* 27.5 (2019): 708-720.
21. Nozha, S. G., Morgan, S. M., Ahmed, S. A., El-Mogazy, M. A., Diab, M. A., El-Sonbati, A. Z., & Abou-Dobara, M. I. "Polymer complexes. LXXIV. Synthesis, characterization and antimicrobial activity studies of polymer complexes of some transition metals with bis-bidentate Schiff base." *Journal of Molecular Structure* 1227 (2021): 129525
22. Prasad, A. S., & K. V. Rao. "Aerobic biodegradation of Azo dye by Bacillus cohnii MTCC 3616; an obligately alkaliphilic bacterium and toxicity evaluation of metabolites by different bioassay systems." *Applied Microbiology and Biotechnology* 97.16 (2013): 7469-7481.
23. Rangappa, Maliyappa M., "Transition metal complexes of ligand 4-imino-3-[(4, 5, 6, 7-tetrahydro-1, 3-benzothiazol-2-yl) diazenyl]-4H pyrimido [2, 1-b][1, 3] benzothiazol-2-ol containing benzothiazole moiety: Synthesis, spectroscopic characterization and biological evaluation." *Inorganic Chemistry Communications* 127 (2021): 108524.
24. Ratnawati, I. G. A. A., Sutapa, G. N., & Ratini, N. N. (2018). The concentration of radon gas in air-conditioned indoor: Air quality can increase the potential of lung cancer. *International Journal of Physical Sciences and Engineering*, *2*(2), 111–119. https://doi.org/10.29332/ijpse.v2n2.169
25. Reddy, V. G., Reddy, T. S., Jadala, C., Reddy, M. S., Sultana, F., Akunuri, R., & Kamal, A. "Pyrazolo-benzothiazole hybrids: Synthesis, anticancer properties and evaluation of antiangiogenic activity using in vitro VEGFR-2 kinase and

in vivo transgenic zebrafish model." *European journal of medicinal chemistry* 182 (2019): 111609.
26. Riswan Ahamed, Mohamed A., Raja S. Azarudeen, & N. Mujafar Kani. "Antimicrobial applications of transition metal complexes of benzothiazole based terpolymer: synthesis, characterization, and effect on bacterial and fungal strains." *Bioinorganic Chemistry and Applications* 2014 (2014).
27. Scardi, Paolo. "Microstructural properties: lattice defects and domain size effects." *Powder Diffraction: Theory and Practice* (2008): 376-413.
28. Seijas, J. A., & M. P. Vázquez-Tato. "Carballido,-Reboredo, M. R; Crecente-Campo, J." *Synlett* 313 (2007).
29. Seth, Sonakshi. "A comprehensive review on recent advances in synthesis & pharmacotherapeutic potential of benzothiazoles." *Anti-Inflammatory & Anti-Allergy Agents in Medicinal Chemistry (Formerly Current Medicinal Chemistry-Anti-Inflammatory and Anti-Allergy Agents)* 14.2 (2015): 98-112.
30. Sharma, Shivani, "Ruthenium catalyzed intramolecular C–S coupling reactions: synthetic scope and mechanistic insight." *Organic letters* 18.3 (2016): 356-359.
31. Sun, Yadong, "Copper-catalyzed synthesis of substituted benzothiazoles via condensation of 2-aminobenzenethiols with nitriles." *Organic letters* 15.7 (2013): 1598-1601.
32. Suryasa, I. W., Rodríguez-Gámez, M., & Koldoris, T. (2022). Post-pandemic health and its sustainability: Educational situation. *International Journal of Health Sciences*, *6*(1), i-v. https://doi.org/10.53730/ijhs.v6n1.5949
33. Wang, Z., Shi, X. H., Wang, J., Zhou, T., Xu, Y. Z., Huang, T. T., & Wei, Y. Q. "Synthesis, structure–activity relationships and preliminary antitumor evaluation of benzothiazole-2-thiol derivatives as novel apoptosis inducers." *Bioorganic & medicinal chemistry letters* 21.4 (2011): 1097-1101.
34. Zheng, Y. Y., Du, R. L., Cai, S. Y., Liu, Z. H., Fang, Z. Y., Liu, T., & Wong, K. Y. "Study of benzofuroquinolinium derivatives as a new class of potent antibacterial agent and the mode of inhibition targeting FtsZ." *Frontiers in microbiology* 9 (2018): 1937.
35. Zhu, X., Zhang, F., Kuang, D., Deng, G., Yang, Y., Yu, J., & Liang, Y. "K2S as sulfur source and DMSO as carbon source for the synthesis of 2-unsubstituted benzothiazoles." *Organic Letters* 22.10 (2020): 3789-3793.